

# DTIC FILE COPY

## REPORT DOCUMENTATION PAGE

Form Approved  
OMB No. 0704-0188

Public reporting burden for this collection of information is estimated to average 1 hour per response, including the time for reviewing instructions, searching existing data sources, gathering and maintaining the data needed, and completing and reviewing the collection of information. Send comments regarding this burden estimate or any other aspect of this collection of information, including suggestions for reducing this burden, to Washington Headquarters Services, Directorate for Information Operations and Reports, 1215 Jefferson Davis Highway, Suite 1204, Arlington, VA 22202-4302, and to the Office of Management and Budget, Paperwork Reduction Project (0704-0188), Washington, DC 20503.

1. AGENCY USE ONLY (Leave blank)	2. REPORT DATE	3. REPORT TYPE AND DATES COVERED Final Report 1 Jan 89-30 Jun 90
----------------------------------	----------------	---

4. TITLE AND SUBTITLE  Research on Materials & Components for Opto-electronic Signal Processing <i>and Computing</i>	5. FUNDING NUMBERS  AFOSR-89-0254 <span style="float: right; border: 1px solid black; border-radius: 50%; padding: 2px;">2</span>
--	---

6. AUTHOR(S) Professor C. Chang	
------------------------------------	--

7. PERFORMING ORGANIZATION NAME(S) AND ADDRESS(ES)  Univ of California Dept of Electrical & Comp Eng, 0407 La Jolla, CA 92093-0407	8. PERFORMING ORGANIZATION REPORT NUMBER  AFOSR-TR- 1171
--	---

9. SPONSORING / MONITORING AGENCY NAME(S) AND ADDRESS(ES)  AFOSR/NE Bldg 410 Bolling AFB DC 20332-6448	10. SPONSORING / MONITORING AGENCY REPORT NUMBER  611027  2305/B4
--	---

11. SUPPLEMENTARY NOTES

**DTIC**  
SELECTE  
DEC 26 1988

12a. DISTRIBUTION / AVAILABILITY STATEMENT  UNLIMITED	12b. DISTRIBUTION CODE
---	------------------------

13. ABSTRACT (Maximum 200 words)

This project is a continuation of the project (AFOSR-84-0389) under the same title "Research on Materials and Components for Opto-Electronic Signal Processing and Computing," for the period Oct 1st, 1984 to Nov. 30th, 1988. A final report for that contract had already been submitted to AFOSR. Therefore, much of the information and data already presented in that report will not be repeated here.

UNCLASSIFIED  
EXEMPT FROM PUBLIC RELEASE  
UNLIMITED

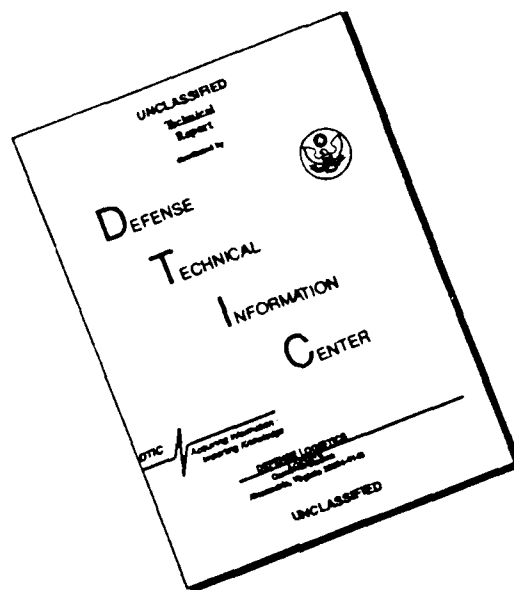
14. SUBJECT TERMS	15. NUMBER OF PAGES
-------------------	---------------------

	16. PRICE CODE
--	----------------

17. SECURITY CLASSIFICATION OF REPORT  UNCLASSIFIED	18. SECURITY CLASSIFICATION OF THIS PAGE  UNCLASSIFIED	19. SECURITY CLASSIFICATION OF ABSTRACT  UNCLASSIFIED	20. LIMITATION OF ABSTRACT
---	--	---	----------------------------

AD-A230 U/I

# DISCLAIMER NOTICE



THIS DOCUMENT IS BEST QUALITY AVAILABLE. THE COPY FURNISHED TO DTIC CONTAINED A SIGNIFICANT NUMBER OF PAGES WHICH DO NOT REPRODUCE LEGIBLY.

**Final Technical Report**

**Research on Materials and Components for Opto-Electronics  
Signal Processing and Computing**

**Sponsored by**

**Air Force Office of Scientific Research  
Air Force Systems Command, USAF  
under grant No. 89-0254**

**submitted by**

**William S. C. Chang (Principal Investigator)  
Shigeru Niki, Albert L. Kellner and H. H. Wieder**

**Department of Electrical and Computer Engineering, 0407  
University of California, San Diego  
La Jolla, CA 92093-0407**

## RESEARCH ON MATERIALS AND COMPONENTS FOR OPTO-ELECTRONIC SIGNAL PROCESSING AND COMPUTING

### 1. Introduction

This project is a continuation of the project (AFOSR 84-0389) under the same title "Research on Materials and Components for Opto-Electronic Signal Processing and Computing." for the period Oct. 1st, 1984 to Nov. 30th, 1988. A final report for that contract had already been submitted to AFOSR. Therefore, much of the information and data already presented in that report will not be repeated here.

Recognizing both the importance of spatial light modulators (SLM) to opto-electronic computing and signal processing and the unique material properties of multiple quantum well (MQW) structures, we have focused our investigation on the electro-optical properties and the growth of  $\text{In}_x\text{Ga}_{1-x}\text{As}/\text{GaAs}$  strained layer material by the molecular beam epitaxy (MBE) method for the SLM's. The potential advantages of the  $\text{In}_x\text{Ga}_{1-x}\text{As}/\text{GaAs}$  SLM are: (1) MQW modulators may be switched with low energy and operated at high speed. (2) Many electronic devices, especially the GaAs MESFET, have already been developed on GaAs. The quality of GaAs substrates is also much higher than that of InP. Thus SLM based on GaAs substrates offer potential advantages in integrating electronic and optical devices for the development of smart SLM. (3) We have demonstrated through this program that thick  $\text{In}_x\text{Ga}_{1-x}\text{As}/\text{GaAs}$  MQW structure for modulators can now be grown with  $0 < x < 0.25$  (or higher). The thicknesses of such structures can exceed substantially the critical layer thickness limitations of pseudomorphic structures. The variations in the composition and well width in such structures allows us to tailor the material property for SLM device optimization, such as tuning the operating wavelength over a wide infra-red range, maximizing the signal to noise ratio, increasing the RC limited bandwidth or minimizing switching voltage. (4) Many lasers now operate in the wavelength range of 0.9 to 1.1  $\mu\text{m}$ , including the  $\text{In}_x\text{Ga}_{1-x}\text{As}$  strained layer QW diode lasers,



A-1

the tunable Ti-sapphire lasers and the high power Nd/YAG lasers at the 1.06  $\mu\text{m}$ . The combination of the high power lasers and SLM constitutes an important advantage in many applications. (5) The GaAs substrate is transparent at wavelengths near the exciton absorption peak, thereby providing a rugged physical bases for the fabrication of complex components.

The research topics that we have investigated during this contract period are directed toward addressing the issues of (a) how to extend the total thickness and the operating wavelength range of  $\text{In}_x\text{Ga}_{1-x}\text{As}/\text{GaAs}$  MQW structure<sup>(1,2,3)</sup> and (b) how to optimize the structural design for SLM's. Specifically we will discuss three topics in the following sections. (1) Growth of a large period of  $\text{In}_x\text{Ga}_{1-x}\text{As}/\text{GaAs}$  QW's with a large InAs mole fraction by using the superlattice and the bulk alloy buffer ( $\text{In}_y\text{Ga}_{1-y}\text{As}$  or  $\text{In}_y\text{Al}_{1-y}\text{As}$ ) interposed between the MQW's and the substrate. (2) The optimization of signal to noise ratio in a SLM. (3) The electro-optical properties of  $\text{In}_x\text{Ga}_{1-x}\text{As}$  superlattices. A much more comprehensive discussion of the materials and the electro-optical properties of the strained layer  $\text{In}_x\text{Ga}_{1-x}\text{As}/\text{GaAs}$  structure for SLM applications is under preparation as S. Niki's Ph.D. Thesis. However, it will not be completed in time to be submitted together with this report, as required by the contract. It will be sent to AFOSR as a supplementary technical report sometime this winter.

## **2. The Growth and the Electro-Optical Properties of Highly-Strained $\text{In}_x\text{Ga}_{1-x}\text{As}/\text{GaAs}$ QW structure**

We have grown strained-layer  $\text{In}_x\text{Ga}_{1-x}\text{As}/\text{GaAs}$  MQW structures with indium compositions of  $0.15 \leq x \leq 0.28$  on GaAs by molecular beam epitaxy (MBE), and investigated the properties of such QW structures with emphasis on their material characteristics intended for surface-normal electroabsorption (EA) modulator applications. The interposition of an appropriate buffer layer between the GaAs substrate and QW structure has made possible the growth of elastically-deformed  $\text{In}_x\text{Ga}_{1-x}\text{As}/\text{GaAs}$  MQWs with the total thickness of the epitaxial layers well beyond the pseudomorphic limit. Optical investigations of such QW structures showed distinct exciton peaks and clear quantum confined Stark effect (QCSE),

indicating good crystalline quality suitable for these device applications. The exciton line can be tuned, up to the wavelength of  $1.09 \mu\text{m}$ , by increasing the indium composition of the ternary alloy.

Three different types of samples have been grown by MBE on (100) oriented GaAs substrates at substrate temperatures between  $500^\circ\text{C}$  and  $530^\circ\text{C}$ . The details of growth parameters are listed in Table 1. Type one has no strained-layer buffer, and type 2 has a superlattice buffer. A superlattice buffer which consists of 125 periods of  $\text{In}_x\text{Ga}_{1-x}\text{As}$  ( $25\text{\AA}$ )/GaAs( $25\text{\AA}$ ) with the same indium concentration as in the  $\text{In}_x\text{Ga}_{1-x}\text{As}$  layers of the QW's was used for sample 3 and 4. In the type 3 sample, an  $\text{In}_{0.13}\text{Ga}_{0.87}\text{As}$  ternary alloy buffer ( $d \sim 500\text{nm}$ ) and a 50-period  $\text{In}_{0.25}\text{Ga}_{0.75}\text{As}(50\text{\AA})/\text{GaAs}(50\text{\AA})$  superlattice buffer were interposed between the GaAs substrate and QWs for sample 6. The ternary compositions and thicknesses of the epitaxial layers were determined by RHEED (reflection high energy electron diffraction), and calibrated by cross-sectional transmission electron microscopy (TEM).

	Type 1	Type 1	Type 2	Type 2	Type 1	Type 3
Sample number	1(473)	2(474)	3(476)	4(514)	5(686)	6(1328)
In Composition	0.15	0.19	0.15	0.22	0.15	0.25
Periods of QWs	80	80	50	50	50	30
Well Width ( $\text{\AA}$ )	120	120	120	120	100	100
Barrier Width ( $\text{\AA}$ )	120	120	120	120	100	100
Buffer Layer	None	None	SL	SL	None	Alloy+SL
Linewidth FWHM (meV)	14.0	23.6	11.4	16.4	13.4	18.0
Wavelength of Exciton Peak ( $\mu\text{m}$ )	0.993	1.021	0.985	1.035	0.962	1.058

Table 1. Comparison of growth parameters and optical characteristics of strained-layer  $\text{In}_x\text{Ga}_{1-x}\text{As}/\text{GaAs}$  multiple quantum well structures

p-i-n diodes with a ring-shaped electrode 300  $\mu\text{m}$  inner diameter and 500  $\mu\text{m}$  outer diameter were fabricated on such samples using standard photolithographic processes. Zn-Au metal contact was used for p-type substrates and Ge-Au contact for n-type substrates. Au/Cr contact was used for the cap layers. Each device was mesa etched to the substrate with a solution,  $\text{H}_3\text{PO}_4 : \text{H}_2\text{O}_2 : \text{H}_2\text{O} = 8 : 1 : 1$  for electrical isolation. I-V traces of such diodes showed small leakage currents, less than  $1\mu\text{A}$ , under the electric field of up to  $F \sim 70\text{-}90\text{kV/cm}$ .

Optical properties of such QW structures were investigated by means of both absorption and EA spectroscopy at room temperature with the input light normal to the substrate. The reflection from the surfaces and residual absorption in the substrate were subtracted from the raw signal by using a reference substrate. The linewidth and wavelength of these exciton peaks are shown in Table 1.

EA characteristics of the samples were measured by applying a DC reverse bias to a p-i-n diode fabricated from such structures. EA spectra obtained from sample 6 are shown in Fig. 1 as an example. The linewidths of the exciton peaks as a function of electric field are shown in Fig. 2. A severe linewidth broadening was observed with increasing of electric field for sample 2, but not for the other specimens. We believe this broadening is due to the enhanced scattering and/or greater tunneling probability with or via deep traps generated by dislocation loops.

A distinct exciton peak with a linewidth of 14meV, which is comparable to those obtained from pseudomorphically grown QWs<sup>(4)</sup>, was observed from sample 1. The linewidth of sample 2 is distinctly larger than those of the other specimens. The smallest linewidth of 11.4 meV was obtained from sample 3. A small linewidth is observed from sample 4 despite the larger lattice-mismatch. This suggests that a superlattice buffer may play an important role in the growth of strained  $\text{In}_x\text{Ga}_{1-x}\text{As}/\text{GaAs}$  QWs. We have tried to grow the QWs categorized in type 1 or 2 using  $x > 0.25$ . However, no exciton peak has been observed. In order to extend the exciton peak to longer wavelengths, a bulk alloy buffer was employed and interposed between the QW and the GaAs substrate. The InAs mole fraction of the alloy buffer is near the average InAs mole fraction of the  $\text{In}_x\text{GaAs}/\text{GaAs}$  MQWs, provided that the strain is well-balanced in the

$\text{In}_x\text{Ga}_{1-x}\text{As}$  and GaAs layer (compressive strain in the  $\text{In}_x\text{Ga}_{1-x}\text{As}$  layer and tensile strain in the GaAs layer). Sharp exciton peak and electroabsorption effect have been measured in sample 6 as shown in Fig. 1. The QW structures with  $x = 0.28$  in type 3 showed sharp exciton peaks at  $\lambda = 1.08\text{-}1.09 \mu\text{m}$ .

The cross-sectional images of the samples were obtained by means of TEM. It was found that misfit dislocations are created within the first few QW periods and no propagating dislocations are found in the remaining active QW layers of sample 1. However, TEM pictures of sample 2 showed dislocations propagating throughout the QW layers, showing a poor crystalline quality. This result is consistent with that obtained from the optical characterization. The strained-layer buffers have successfully confined misfit dislocations at the superlattice/GaAs interface for sample 3 and 4 and the ternary alloy/GaAs interface for sample 6. Therefore, most of the QW layers are elastically deformed.

Double crystal X-ray diffraction was used for investigating the strain relief in these MQW structures. X-ray rocking curves obtained from those samples show several distinct satellite peaks, indicating well-ordered periodic structures. Preliminary analyses indicate large lattice relaxation in the epitaxial layers, provided that each QW layer shares the strain; compressive strain in the  $\text{In}_x\text{Ga}_{1-x}\text{As}$  layers and tensile strain in the GaAs layers.

In summary we have successfully grown  $\text{In}_x\text{Ga}_{1-x}\text{As}/\text{GaAs}$  ( $0.15 \leq x \leq 0.28$ ) MQWs with the total thickness of the strained layer well above the critical layer thickness limit defined for pseudomorphically grown InGaAs on GaAs. Material investigations of such QW structures suggest potential applications for surface-normal EA modulators in the  $0.9\text{-}1.1 \mu\text{m}$  wavelength range. In S. Niki's Ph.D Thesis we will discuss how to specify the composition  $x$  and the well thickness  $L_z$  so that the SLM will operate at a given wavelength.

### 3. Optimization of Strained-Layer MQW Structures for Electro-Absorption SLM

The investigation of material properties of InGaAs/GaAs strained-layer MQW structures discussed in Section 2 made possible the growth of large number of QWs above the pseudomorphic thickness limit for a given In concentration. The exciton absorption peak is shifted in energy and reduced in strength when an electric field is applied, called the quantum confined Stark effect (QCSE). Two kinds of electro-absorption (EA), positive and negative EA can be used to make a modulator. When the wavelength of the input light is slightly longer than (or equal to) that of the exciton peak, the absorption coefficient is increased (decreased) with the increase of electric field, and it is called a positive (negative) EA. Both the negative and the positive EA have been used for SLM's.

Several methods, such as the use of Fabry-Perot resonator, have been discussed in the literature in order to obtain large contrast ratio in GaAlAs/GaAs MQW SLM<sup>(5,6)</sup>. However for SLM with a large residual absorption, the dynamic range of a modulator is determined by the signal to noise ratio. The optical signal is  $I_0\Delta T$  (or  $I_0\Delta R$ ) where  $I_0$  is the input light intensity and  $\Delta T$ (or  $\Delta R$ ) is the change in transmittance (or reflectance) of the modulator. Therefore we have investigated how to optimize  $\Delta T$  (or  $\Delta R$ ), i.e. the dynamic range. In terms of the residual absorption per well (i.e.  $\alpha_0$ ), the change in absorption per well due to QCSE (i.e.  $\Delta\alpha$ ) and the number of QW (i.e.  $n$ ),  $\Delta T$  is given by

$$\Delta T = \Delta I_t / I_0 = \exp(-\alpha_0 \cdot n) [1 - \exp(-\Delta\alpha \cdot n)] \quad (1)$$

The change in reflection ( $\Delta R$ ) is given by

$$\Delta R = R \exp(-2\alpha_0 \cdot n) [1 - \exp(-2\Delta\alpha \cdot n)] \quad (2)$$

where  $R$  is the reflection coefficient of the back surface. In comparison, the contrast ratio is given by  $T_{\max}/T_{\min}$  or  $R_{\max}/R_{\min}$  which is dependent only on  $\exp(-\Delta\alpha \cdot n)$  or  $\exp(-2\Delta\alpha \cdot n)$ . Clearly that the optimization of contrast ratio and the optimization of the signal to noise ratio is not identical to each other.

Theoretically we can obtain an optimum  $n$  that will yield maximum  $\Delta T$  (or maximum  $\Delta R$ ). Any further increase in  $n$  will enhance the contrast ratio, but it will reduce the signal to noise ratio. At the optimum  $n$ , the  $\Delta T_{\max}$  (or  $\Delta R_{\max}$ ) is dependent only on the ratio of  $\Delta\alpha/\alpha_0$ . Any further enhancement of the signal to noise ratio can only be obtained by improving the  $\Delta\alpha/\alpha_0$  of the material.

Calculated  $\Delta T$  and  $\Delta R$  as a function of the period of QWs are shown in Fig. 3(a) for negative EA and Fig. 3(b) for positive EA. The solid curve indicates the calculated  $\Delta T$ , and the dotted curves represent the calculated  $\Delta R$  for reflection mode devices using reflectors, assuming  $R = 0.65$  and  $R = 1$ . For these curves, we have used the  $\Delta\alpha$  and  $\alpha_0$  obtained from sample 5 at the wavelength of  $0.961 \mu\text{m}$  and  $0.972 \mu\text{m}$  for negative and positive EA, respectively, under the electric field,  $5.45 \times 10^4 \text{ V/cm}$ . At this wavelength and electric field,  $\Delta T$  is about maximum for sample 5. This result suggest that reflection type modulators, in which the optical path length is doubled, do not lead to  $(\Delta I_r/I_0)_{\max} > (\Delta I_t/I_0)_{\max}$ . However, they can provide a smaller driving voltage for a given  $(\Delta I_r/I_0)$  if the reflection is large. Therefore, from the point of view of maximizing the dynamic range, there is no special advantage in using a reflection type modulator.

The scatter points show the experimentally measured maximum  $\Delta T$  and  $\Delta R$  of various modulators, including the results obtained from AlGaAs/GaAs MQWs<sup>(7,8,9)</sup>. However, they are not normalized in terms of the electric field and operating wavelength. The effect of well width on EA characteristics is also shown in Fig. 3(a) and (b). Each data point designated as numbers 1-3 is taken from Jelley et al.<sup>(8)</sup> and as A-F taken from Whitehead et al.<sup>(9)</sup> corresponds to a different well width. sample 1, 3, and 5 show comparable or even larger negative EA than AlGaAs/GaAs QWs. On the contrary, Fig. 3(b) shows that much larger  $\Delta T$  is obtained from AlGaAs/GaAs QWs for positive EA. It is also clear that thinner QWs provide larger  $\Delta T$  for positive EA.

The data obtained by Bailey et al.<sup>(7)</sup> indicates that a larger  $\Delta I_r/I_0$  is obtained from a transmission type modulator than  $\Delta I_t/I_0$  of a reflection type with same number of QWs for both

positive and negative EA. This occurs despite the maximum contrast ratio of the reflection type modulator is much higher than that of transmission type; for example, 26.1:1 (reflection type) and 4.4:1 (transmission type) for positive EA. As we mentioned earlier the dynamic range of a modulator can not be optimized by maximizing the contrast ratio.

The preceding results indicate that reasonably large EA has already been obtained from strained-layer  $\text{In}_x\text{Ga}_{1-x}\text{As}/\text{GaAs}$  MQW modulators. The dynamic range is more effectively enhanced by increasing the input optical power and by reducing the receiver noise power. In the case of modulators used in analogue systems, the linearity of the modulator may be a more important consideration than the maximum  $\Delta T$  and  $\Delta R$ . However,  $\Delta T$  or  $\Delta R$  should still be maximized at a given voltage. A more detailed discussion on the optimization of the design will be presented in S. Niki's Thesis.

QW modulators may be improved by optimizing the intrinsic characteristics of QCSE by changing the width and depth of the potential wells. Because the exciton peak is shifted in energy and reduced in strength with increasing electric field ( $F$ ),  $\Delta T$  and  $\Delta R$  at a given voltage will be maximized by optimizing three parameters, the linewidth ( $\Delta\Gamma$ ), the energy shift of the exciton peak ( $\Delta E$ ), and the change in oscillator strength ( $\Delta f/f_0$ ).  $\Delta T$  and  $\Delta R$  are very sensitive to  $\Delta\Gamma$ . Practically speaking, it is very difficult to control  $\Delta\Gamma$  because it is strongly dependent on the material quality. Therefore, it should be kept as small as possible. The continuous absorption plateau and excitonic absorption peak which usually overlap, make it difficult to reduce the residual absorption for negative EA in practice. On the other hand,  $\Delta T$  or  $\Delta R$  can be improved for positive EA by optimizing  $\Delta E$  and  $\Delta f/f_0$ , both of which are functions of  $L_z$  and the depth of the potential wells ( $\Delta E_c$ ,  $\Delta E_v$ ).

Fabry-Perot etalon may produce an improvement in  $\Delta T$  and  $\Delta R$ . However, the complication attendant on the use of mirrors and the requirement for tight control of tolerances of the etalon must be weighted in balance against the potential advantages of such devices.

#### 4. Electroabsorption Properties of Strained-Layer $\text{In}_x\text{Ga}_{1-x}\text{As}/\text{GaAs}$ Superlattices

We have investigated the electroabsorption (EA) effects of strained-layer  $\text{In}_x\text{Ga}_{1-x}\text{As}/\text{GaAs}$  superlattices (SLs) because of the following reasons. First high quality strained-layer  $\text{In}_x\text{Ga}_{1-x}\text{As}/\text{GaAs}$  multiple quantum wells (MQWs) have been grown on GaAs by interposing an  $\text{In}_x\text{Ga}_{1-x}\text{As}/\text{GaAs}$  SL between the GaAs and the MQW region<sup>(3)</sup>. Second, novel EA effects which provide large absorption change have been reported recently in the SL structures using the Wannier-Stark localization effect<sup>(10,11)</sup>, and such SL structures have been utilized for surface-normal EA modulator applications<sup>(12)</sup>.

All the specimens have been grown by molecular beam epitaxy on (100)-oriented GaAs substrates at  $T_s = 500\text{--}530^\circ\text{C}$ . P-i-n diodes with a ring-shaped electrode  $300\ \mu\text{m}$  inner diameter and  $500\ \mu\text{m}$  outer diameter were fabricated on such SL structures. Sample 1 consists of a 125-period  $\text{In}_{0.19}\text{Ga}_{0.81}\text{As}(25\text{\AA})/\text{GaAs}(25\text{\AA})$  layer grown on a GaAs buffer. Sample 2 consists of a 50-period  $\text{In}_{0.25}\text{Ga}_{0.75}\text{As}(50\text{\AA})/\text{GaAs}(50\text{\AA})$  layers grown on a  $0.5\ \mu\text{m}$ -thick  $\text{In}_{0.13}\text{Ga}_{0.87}\text{As}$  buffer layer. Cross-sectional images of similar structures showed that the misfit dislocations are confined at the GaAs/strained-layer interface, thereby most of the active region is dislocation free<sup>(3,13)</sup>.

Wannier-Stark localization effect has not been observed in strained-layer  $\text{In}_x\text{Ga}_{1-x}\text{As}/\text{GaAs}$  system. It may be due to smaller band offsets and/or interface roughness associated with the strained-layer growth. We have increased the InAs mole fraction of the ternary layers up to  $x = 0.25$  in order to reduce the width of the minibands.

EA spectra obtained from sample 1 and 2 are shown in Figs. 4 and 5, respectively. Fig. 5 shows a blue shift of the absorption edge under the electric field,  $2.2 \times 10^4 < F < 4.4 \times 10^4$  (V/cm), which is in accord with a simple Kronig-Penney calculation ( $\Delta_e = 28$  meV), suggesting a decoupling of ground-state electron miniband. On the other hand, EA in sample 1 is considered to be similar to that of the bulk material and is attributed to photon-assisted tunneling between the ground-state electron and heavy-hole minibands.

We have shown that the EA of the  $\text{In}_x\text{Ga}_{1-x}\text{As}/\text{GaAs}$  SLs could vary from that similar to bulk material to that exhibiting a blue shift, depending on the structure. Further optimization may provide various device applications in this spectrum range.

## 5. Papers Published and Presented

1. T. E. Van Eck, S. Niki, P. Chu, W. S. C. Chang, H. H. Wieder, A. J. Mardinly, K. Aron and G. A. Hansen, "Strained Superlattice Buffer Layer for InGaAs/GaAs Quantum Wells". Presented at the Topical Meeting on Quantum Wells for Optics and Optoelectronics, Salt Lake City, March, 1989.
2. M. K. Chin, S. Niki, S. C. Lin, P. K. L. Yu, W. S. C. Chang, and S. Thaniyavarn, "Electroabsorption Modulators Using InGaAs/GaAs Multiple Quantum Well and Superlattice Waveguides at  $0.93 \mu\text{m}$ ". Presented at the LEOS 1989, Orlando, Florida, Oct. 17-20, 1989
3. C. C. Sun, H. H. Wieder, and W. S. C. Chang, "A New Semiconductor Device - The Gate - Controlled Photodiode: Device Concept and Experimental Results". *IEEE J. of Quantum Electronics* **25**(5), 896-903 (1989)
4. S. Niki, C. L. Lin, W. S. C. Chang and H. H. Wieder, "Band-edge discontinuities of strained layer  $\text{In}_x\text{Ga}_{1-x}\text{As}/\text{GaAs}$  heterojunctions and quantum wells". *Appl. Phys. Lett.*, **55**(13), 1339 (1989).
5. S. C. Lin, P. K. L. Yu, S. Niki and W. S. C. Chang, "Chirping of electroabsorption modulation". *SPIE Optical Technology for Microwave Applications IV*, **1102** 30 (1989).
6. S. Niki, A. L. Kellner, S. C. Lin, A. Cheng, A. R. Williams, W. S. C. Chang, and H. H. Wieder, "Electroabsorption effects in  $\text{In}_x\text{Ga}_{1-x}\text{As}/\text{GaAs}$  strained-layer superlattices". *Appl. Phys. Lett.* **56**(5), 475 (1990).
7. S. Niki, H. H. Wieder, and W. S. C. Chang, "Optimization of Strained  $\text{In}_x\text{Ga}_{1-x}\text{As}/\text{GaAs}$  Quantum Wells for Electroabsorption Modulation". Presented at the SPIE Digital Optical

Computing II O-E Lase '90, January 14-19 1990, Los Angeles, CA. Published in the SPIE Vol. 1215 Digital Optical Computing II, 235 (1990).

8. T. E. Van Eck, K. P. Aron, G. A. Hansen, R. S. Lytel, S. Niki, W. S. C. Chang and H. H. Wieder. "Nonlinear Absorption In a Strained InGaAs/GaAs MQW/n-i-p Structure". Presented at the NLO '90 Conference., July 16, 1990, Kanai, Hawaii
9. S. Niki, H. H. Wieder, and W. S. C. Chang, "Surface-Normal Electroabsorption Modulators in the 0.9-1.1  $\mu\text{m}$  Wavelength Range", Presented at the LEOS '90, November 4-8, 1990, Boston, MA.
10. S. Niki, A. Cheng, W. S. C. Chang, and H. H. Wieder, "Properties of Highly-Strained  $\text{In}_x\text{Ga}_{1-x}\text{As}/\text{GaAs}$  Multiple Quantum Wells". Presented at the Materials Research Society Meeting, November 26-December 1, 1990, Boston, MA.
11. Shigeru Niki, An-Nien Cheng, Jessica C. P. Chang, William S. C. Chang, and Harry H. Wieder, "Highly-Strained  $\text{In}_x\text{Ga}_{1-x}\text{As}/\text{GaAs}$  Multiple Quantum Wells for Electroabsorption Modulation", to be published in the *Japanese J. Appl. Phys.*.
12. S. Niki, W. S. C. Chang, H. H. Wieder, and T. E. Van Eck, "Molecular Beam Epitaxial Growth and Properties of Highly-Strained  $\text{In}_x\text{Ga}_{1-x}\text{As}/\text{GaAs}$  Multiple Quantum Wells", presented at the 6th International Conference on Molecular Beam Epitaxy, August 26-31, 1990, San Diego, CA.; to be published in the *J. Cryst. Growth.*

## 6. References

- (1) U. Das, P. R. Berger, and P. Bhattacharya, *Opt. Lett.*, **12**, 820 (1987).
- (2) U. Das, Y. Chen, P. K. Bhattacharya, and P. R. Berger, *Appl. Phys. Lett.*, **53**, 2129 (1988).
- (3) S. Niki, H. H. Wieder, and W. S. C. Chang, SPIE Vol. 1215, *Digital Optical Computing II*, 235 (1990).

- (4) D. A. Dahl, L. J. Dries, F. A. Junga, W. G. Opyd, and P. Chu, *J. Appl. Phys.* **61**, 2079 (1987).
- (5) G. D. Boyd, D.A. B. Miller, D. S. Chemla, S. L. McCall, A. C. Gossard, and J. H. English, *Appl. Phys. Lett.* **50**, 1119 (1987).
- (6) R. H. Yan, R. J. Simes, and L. A. Coldren, *IEEE Photonics Technol. Lett.* **1**, 273 (1989).
- (7) R. B. Bailey, R. Sahai, and C. Lastufka, presented at the Quantum Wells for Optics and Optoelectron.: Topical Meeting, Salt Lake City, Utah, 1989, paper PD1-1.
- (8) K. W. Jelley, R. W. H.Engelmann, K. Alavi, and H. Lee, *Appl. Phys. Lett.*, **55**, 70 (1989).
- (9) M. Whitehead, P. Stevens, A. Rivers, G. Parry, J. S. Roberts, P. Mistry, M. Pate, and G. Hill, *Appl. Phys. Lett.* **53** 956 (1988).
  
- (10) R. H. Yan, R. J. Sims, H. Ribot, L. A. Coldren, and A. C. Gossard, *Appl. Phys. Lett.* **54**, (1989).
- (11) J. Bleuse, P. Voisin, M. Allovon, and M. Quillec, *Appl. Phys. Lett.* **53** 2632 (1988).
- (12) K.-K. Law, R. H. Yan, J. L. Merz, and L. A. Coldren, *Appl. Phys. Lett.* **56**, 1886 (1990).
- (13) S. Niki, A. Cheng, J. C. P. Chang, W. S. C. Chang, and H. H. Wieder, to be published in *Jpn. J. Appl. Phys.* **29**, no. 10 (1990).

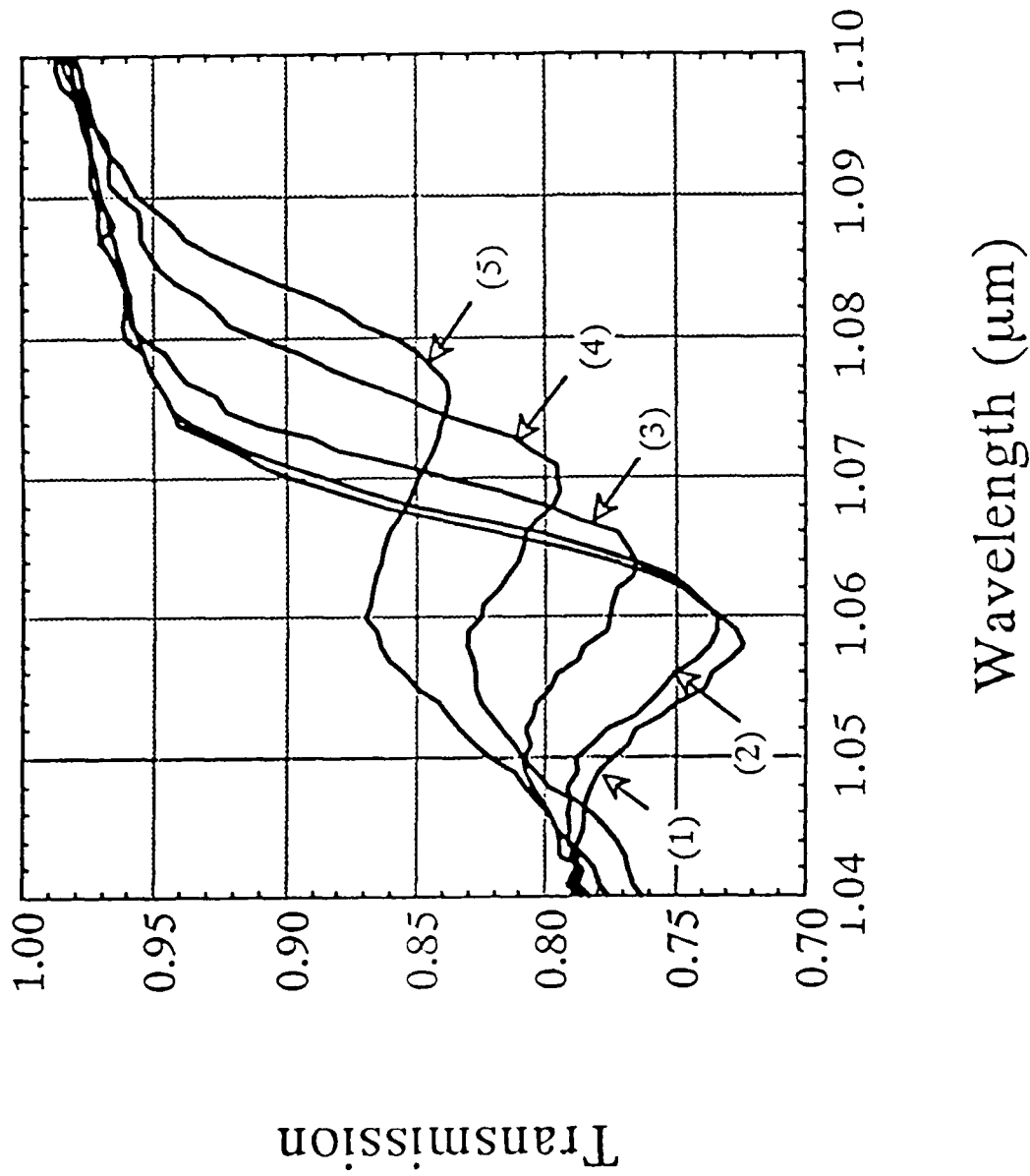


Figure 1.  
 Electroabsorption spectra obtained from sample 6. (1)-(5) correspond to electric fields of 0, 2.2, 4.4, 6.7, and 8.8 ( $\times 10^4$  V/cm).

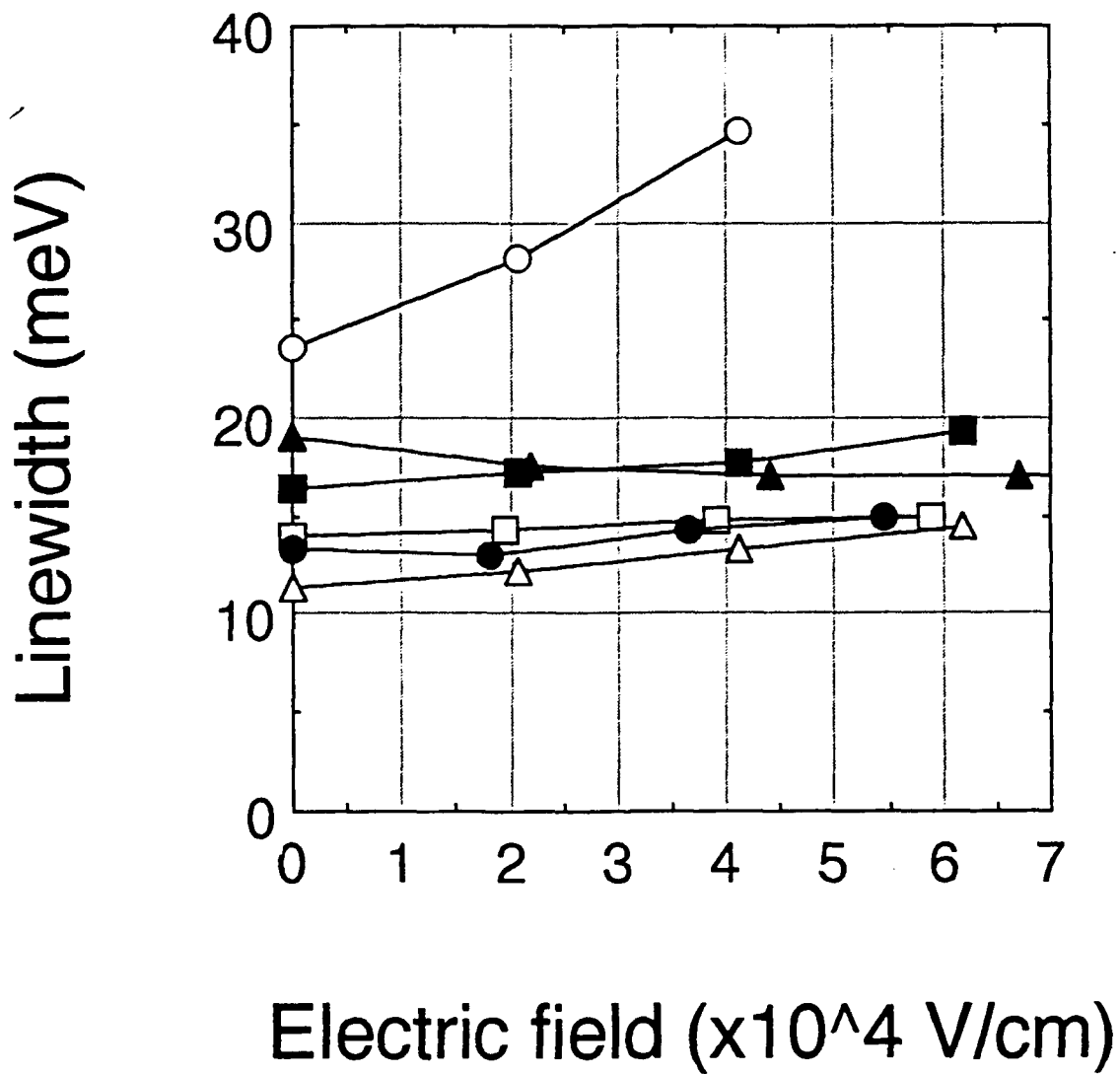
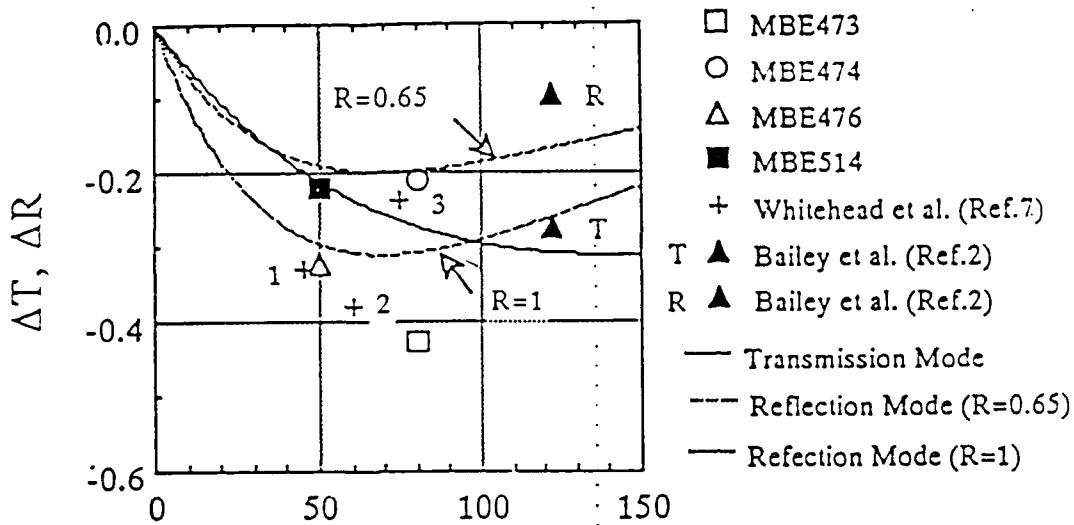
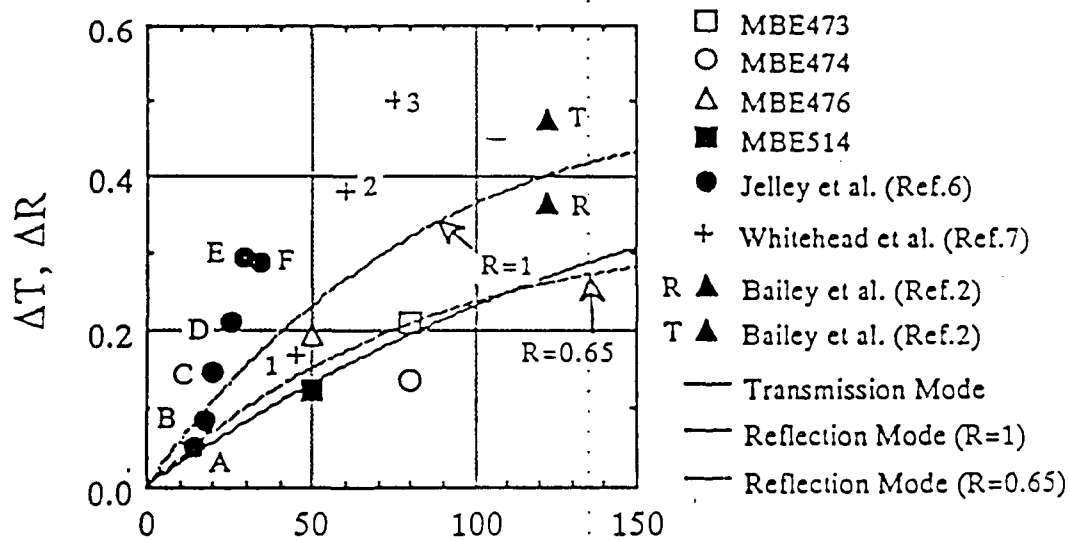


Figure 2.  
 Linewidth of exciton peaks as a function of electric field. □: sample 1,  
 ○: sample 2, △: sample 3, ■: sample 4, ●: sample 5, ▲: sample 6.



(a) The Number of Periods



(b) The Number of Periods

Figure 3.

(a)  $\Delta T$  and  $\Delta R$  for negative electroabsorption (b)  $\Delta T$  and  $\Delta R$  for positive electroabsorption; solid curves represent the calculated  $\Delta T$ , and dotted curves indicate the calculated  $\Delta R$ . + 1-3 correspond to well widths of  $L_z = 147 \text{ \AA}$ ,  $87 \text{ \AA}$ , and  $47 \text{ \AA}$  respectively.  $\Delta T$  and  $\Delta R$  indicate transmission and reflection type.  $\bullet$  A-F correspond to  $L_z = 260 \text{ \AA}$ ,  $202 \text{ \AA}$ ,  $155 \text{ \AA}$ ,  $105 \text{ \AA}$ ,  $75 \text{ \AA}$ ,  $50 \text{ \AA}$  respectively.

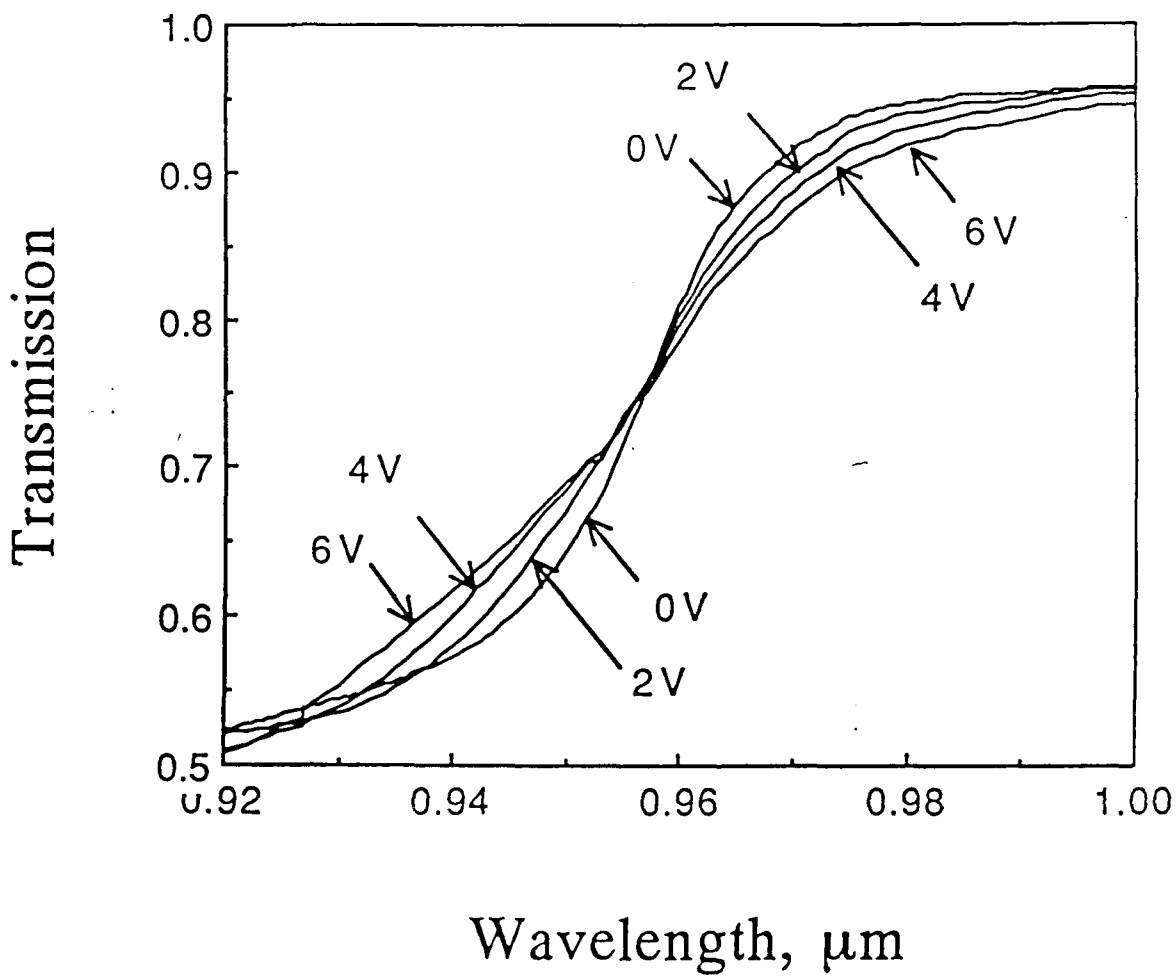


Figure 4.  
Electroabsorption spectra obtained from sample 1.

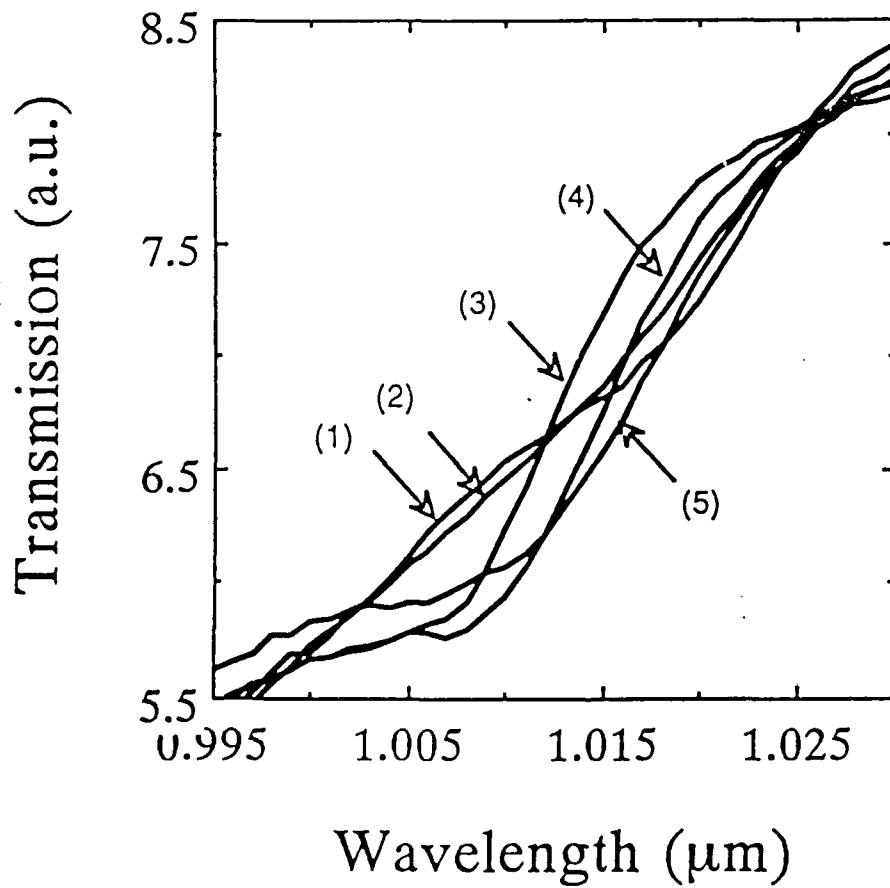


Figure 5.  
Electroabsorption spectra obtained from sample 2.  
(1)-(5) correspond to electric fields of  $F=0, 2.2, 4.4, 6.7$  and  $8.9 \times 10^4$  (V/cm).